STUDY ON WATER DEPOSIT IN RAPID FREEZE PROTOTYPING PROCESS

G. Sui, W. Zhang, and M.C. Leu

Department of Mechanical and Aerospace Engineering and Engineering Mechanics
University of Missouri – Rolla, MO 65409-0050
E-mail: mleu@umr.edu

Abstract

Rapid Freeze Prototyping (RFP) builds a three-dimensional ice part according to its CAD model by depositing and rapidly freezing water in a layer-by-layer manner. To study the water deposit in RFP, assumptions are made based on the deformation of water droplet impinging on a flat substrate, the thermal analysis of a new layer of water deposit, and the characteristics of solidification of a water drop. The equations governing the cross-sectional profile of the water deposit are then established. A model of water deposit is proposed by simplifying the equations under our experimental conditions in RFP. By using this model, equations for layer thickness of vertical and slant walls built by RFP are derived and verified by experiments.

1. Introduction

Rapid Freeze Prototyping (RFP) is one of the solid freeform fabrication (SFF) techniques [1]. RFP builds a three-dimensional ice part according to its CAD model by depositing and rapidly freezing water in a layer-by-layer manner. Compared with other SFF processes, it has many advantages including cheaper equipment and material, cleaner material and process, less energy consumption, faster building speed and better surface finish. Figure 1 shows the overall setup of RFP process and close-up of the process around the nozzle. The ice part building process is conducted in the freezer. After being ejected from the drop-on-demand nozzle, water droplets deposit on the substrate or previously formed layer of ice. On the substrate, water droplets do not solidify immediately. Instead, they unite together to become part of the continuous water line, which is called the water deposit. During the RFP process, newly ejected water droplets continuously join the water deposit. Meanwhile, the water deposit changes phase to ice continuously.

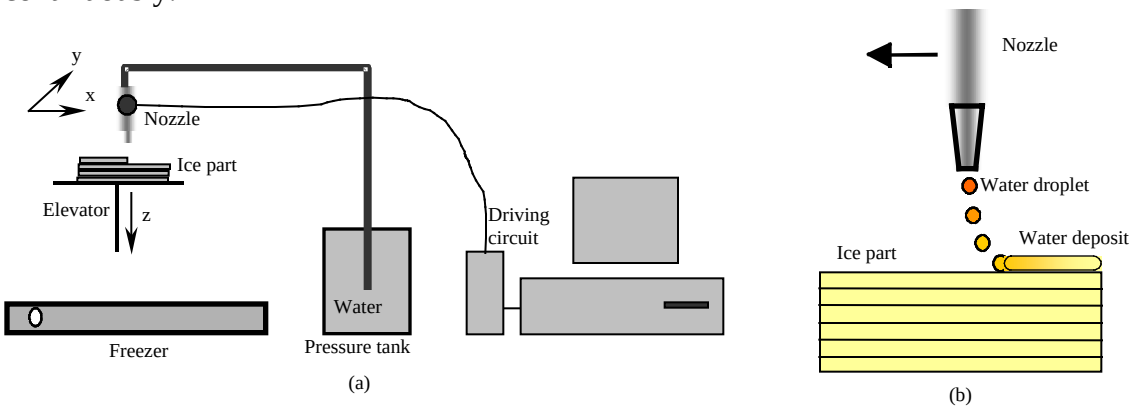

Figure 1 Principle of Rapid Freeze Prototyping

There has been no study on the water deposit formation and solidification in the RFP process. However, the phenomenon of a single water droplet impinging on a flat substrate without solidification has been well studied [2-4]. For example, Figure 2 shows the deformation

of a water droplet with diameter of 0.1mm [2]. Generally speaking, the deformation process of a water droplet impinging on a flat substrate lasts for only 1-10 milliseconds.

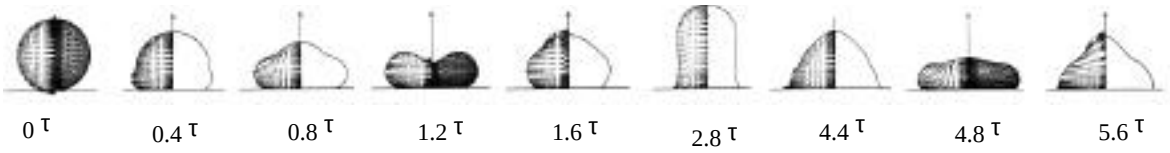

Ro = 0.1mm, V = 1m/s, τ = 0.1ms

Figure 2 Deformation of a single droplet impinging a flat substrate [2]

Figure 3 shows the result of a water drop solidifying on a cold plate studied by Daniel Anderson [5]. Although the water drop initially of spherical shape has solidified into an ice drop with a cusp-like top, the water drop keeps its initial shape at the early stage of solidification.

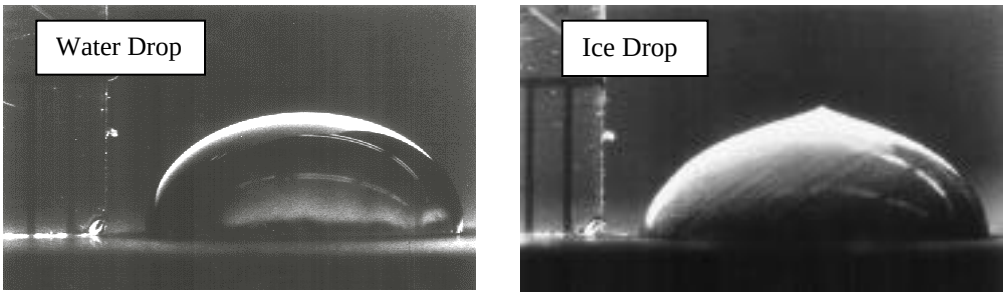

(a) (b)

Figure 3 Solidification of water drop on a cold plate [5]

We have studied the solidifying time of a newly formed layer of water [6]. Under the current RFP experimental condition, from both the observation of the process and the thermal analysis of forming the new layer, the time needed to solidify the new layer is in the order of 0.1-1 second.

Layer thickness is one of the most important parameters of all SFF processes. There are many factors that affect the layer thickness in RFP. However, only scanning speed v (mm/s) and water feed rate f (mm^3/s) are the parameters that can be changed in our present RFP apparatus. In the following section, the governing equations of the cross-sectional profile of water deposit are established and a model of water deposit is proposed by simplifying the equations based on our experimental conditions.

2. Water Deposit Model

After a water droplet touches the substrate, it becomes part of the continuous water deposit. Meanwhile, it starts freezing. This is a coupled deformation and solidification problem. However, since the deformation of a single droplet takes a very short time, we make our first assumption:

Before solidification begins, the water deposit achieves its balance state quickly and its shape is well defined.

The water drop keeps its initial shape in the early solidification stage. Again, from our experimental observation of water drop, we make another assumption of water deposit:

The water deposit keeps its shape during the solidification process.

With the two assumptions above, the coupled deformation and solidification problem can be considered separately. The final profile of the deposit is thus independent of the solidification process.

Figure 4 (a) illustrates the water deposit on a flat substrate. Figure 4 (b) shows the coordinate system describing the cross-sectional profile of the water deposit where α is water-substrate contact angle and z_h is the total height of water deposit. We take a small element with the length of *dl* in longitudinal direction as shown in Figure 4 (c) to analyze the force equilibrium of the boundary element [7].

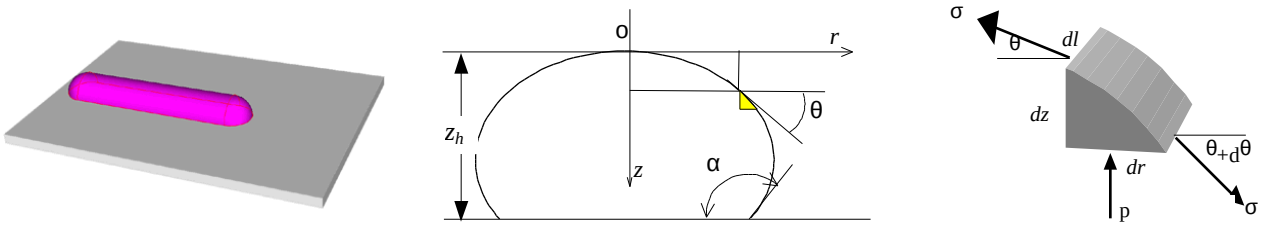

(a) Water deposit on a plate (b) Cross-section of water deposit (c) A small element

Figure 4 Water deposit illustration

Since this small element is in equilibrium, the upward force due to the internal liquid pressure and surface tension is:

$$F_{up} = p \ \ dldr + \sigma \sin(\theta) \ \ dl$$

where *p* is the liquid pressure just under the element and σ is water's surface tension. From hydrostatics and properly applying Young-Laplace equation, the pressure *p* can be expressed as:

$$p = \rho g z + \frac{\sigma}{R_0} \qquad (1)$$

where ρ is the water density, *g* is gravity and R_0 is the radius of curvature at the apex.
The downward force due to surface tension is:

$$F_{down} = \sigma \sin(\theta + d\theta) \ \ dl$$

Equilibrium requires that $F_{down} = F_{up}$, so we have

$$\sigma \sin(\theta + d\theta) \ \ dl = p \ \ dldr + \sigma \sin(\theta) \ \ dl \qquad (2)$$

Since $\sin(\theta + d\theta) \quad \sin(\theta) + \cos(\theta) d\theta$, equation (2) can be finally simplified as

$$\frac{dr}{d\theta} = \frac{\sigma \cos\theta}{\rho g z + \sigma / R_0} \qquad (3)$$

Also, from Figure 4 (c),

$$\frac{dz}{d\theta} = \tan(\theta)\frac{dr}{d\theta} = \frac{\sigma \sin\theta}{\rho g z + \sigma / R_0} \qquad (4)$$

Equations (3) and (4) are the governing differential equations whose solution gives the profile of the water deposit. We can get the analytical solution of equation (4) as follows:

$$z = \frac{\sqrt{(\sigma / R_0)^2 + 2\rho g\sigma(1 - \cos\theta)} - \sigma / R_0}{\rho g} \qquad (5)$$

The analytical solution of equation (3) is very complicated and involves elliptical integration. We will not discuss it in this paper.

To solve the governing equations, we have the following initial and boundary conditions:

at the apex, where $\theta = 0$,

$$z = 0, \quad r = 0, \quad \frac{dr}{d\theta} = R_0, \quad \frac{dz}{d\theta} = 0$$

at $\theta = \alpha$,

$$\int_0^{\alpha} \int_0^{\theta} \frac{\sigma \cos t}{\rho g z(t)} dt \; d\theta = \int_0^{z_h} r dz = \frac{1}{2} A$$

where A is the cross-sectional area of the water deposit.

Given the apex radius R_0 and contact angle α, the governing equations along with these conditions can be solved by a numerical method. Figure 5 shows some water deposit profiles calculated by the governing equations with 180° contact angle and different apex radii.

R_0=10mm *R_0=1mm* *R_0=0.45mm (Experimental condition)*

Figure 5 Different water deposit profiles calculated by the governing equations

From the three cases we can see that the smaller the apex radius R_0, the rounder its shape. We may compare the radius of curvature at $\theta=90°$ with the radius of curvature at $\theta=0$, which is R_0. The radius of a curve can be derived with equation (6) if the curve is written in the form of $y=f(x)$.

$$R = \frac{\left[1 + (dy/dx)^2\right]^{3/2}}{d^2y/dx^2} \qquad (6)$$

By applying equation (6), the radius at any given angle θ can be derived as:

$$R = \left(\frac{1}{R_0^2} + 2\frac{\rho g}{\sigma}(1 - \cos\theta)\right)^{-\frac{1}{2}} \qquad (7)$$

Clearly, R has the smallest value at $\theta=90°$ where is the right-most or left-most side of the profile. The radius at apex R_0 is used as a variable to see its effect on the roundness of the profile of water deposit. Figure 6 shows the radius at $\theta=90°$ vs. the radius at the apex.

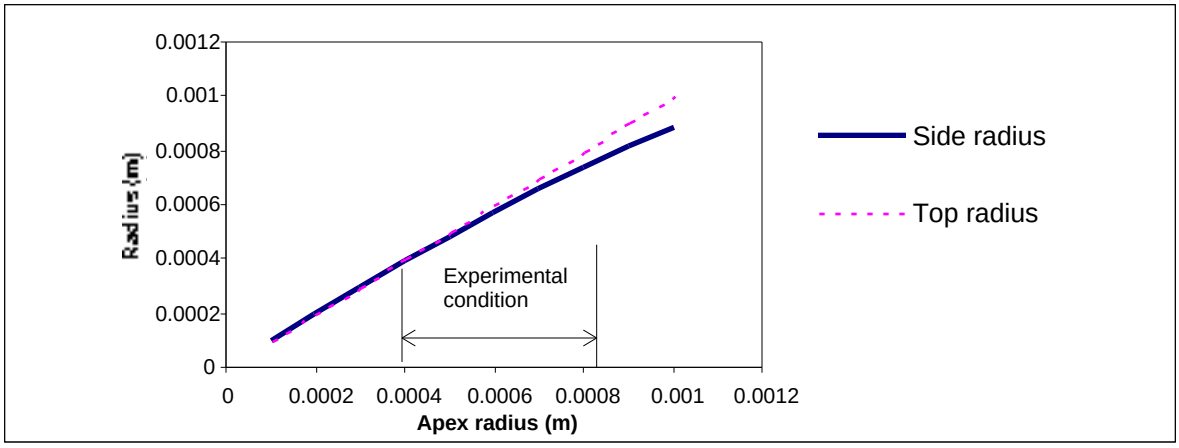

Figure 6 Comparison of apex radius and left-most side radius

If the apex radius is very small, the side radius is essentially equal to the apex radius. That means its profile is circular. However, if the apex radius increases, the difference between the apex radius and the side radius increases too. Within our experimental conditions, the maximum deviation of the side radius from the apex radius is about 9%. Under the normal condition where the apex radius is around 0.5mm, the deviation is only 3%. Thus the profile of water deposit is almost circular.

Due to the roundness of cross-section of water deposit under our experimental condition, we use a simplified model for the shape of water deposit as follows: *The profile of water deposit cross-section is circular.* The layer thickness of vertical and slant walls will be discussed using the simplified model in the following sections.

3. Vertical Wall Building

With the initial and boundary conditions of equations (3) and (4), the profile of water deposit can be determined by cross-section area A and contact angle α. But how do the processing parameters such as scanning speed v and water feed rate f relate to cross-section A?

Assume that the water deposit is uniform along the longitudinal direction. If the nozzle moves at speed v, in a certain time t the length of water deposit is vt. So the volume of the newly generated water deposit is Avt. On the other hand, the volume of the water deposit can also be calculated as ft. Thus,

$$A = f / v \qquad (8)$$

In the RFP process, if we change processing parameters such as water feed rate f and/or scanning speed v, the layer thickness Δz changes accordingly.

When a vertical wall is built, after many layers, say n layers, the profile of layer n+1 should be identical to that of layer n. Figure 7 illustrates this. The cross-sectional profile of water deposit is circular according to the model proposed in Section 2. A is area of shaded layer, α is water-ice contact angle, Δz is layer thickness and W is line width. Because the outline of each water deposit is circular, we can easily get the relation between layer thickness and line width as follows:

$$\Delta z = W \sin(\frac{\alpha}{2}) \qquad (9)$$

Along with the relation that $A = f / v = W \cdot \Delta z$, the layer thickness and line width can be derived as:

$$\Delta z = \sqrt{\frac{f \sin(\alpha / 2)}{v}} \qquad (10)$$

$$W = \sqrt{\frac{f}{v \sin(\alpha / 2)}} \qquad (11)$$

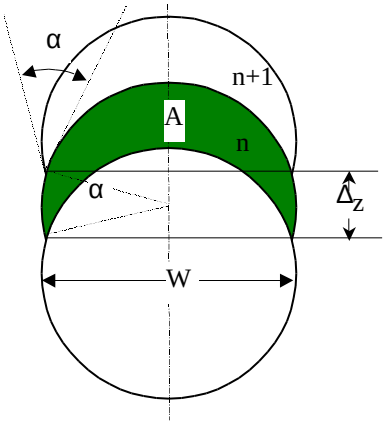

Figure 7 Illustration of vertical wall

The results show that the layer thickness and line width of a vertical wall are purely determined by scanning speed, water feed rate, and water-ice contact angle. The water-ice contact angle should be constant under certain conditions. However, the value of water-ice contact angle is quite different as reported in various references [8-11], mainly because it is small and difficult to measure. Figure 8 shows experimental data and the predicted values of layer thickness if we take the contact angle as 20°. The predictions agree with the experimental data very well.

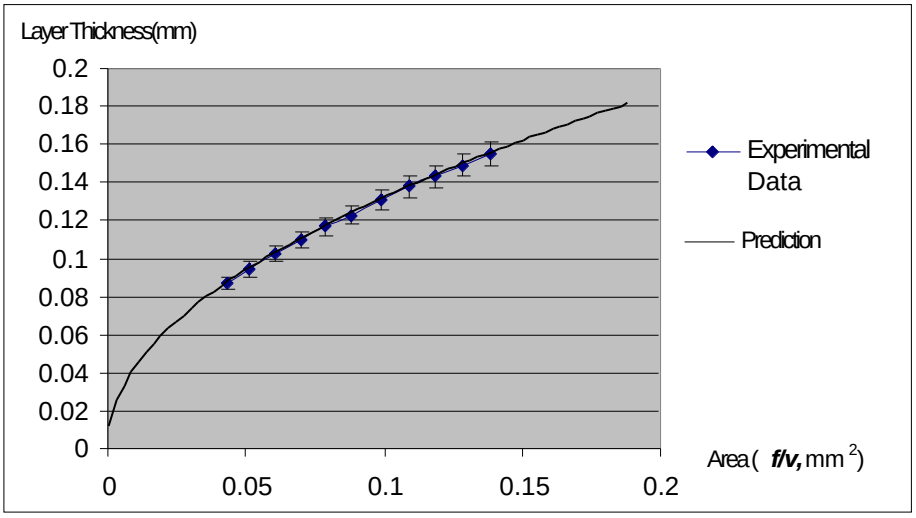

Figure 8 Layer thickness: experimental data vs. model predictions

4. Slant Wall Building

Figure 9 (a) shows a slant wall. To build a slant wall, each new layer offsets a certain distance Δx.

In building a slant wall, because the new layer is not built vertically upon the previous layer, the average layer thickness in Z direction is less than that of a vertical wall. This can be seen in Figure 9 (b). As a result, the top surface is not flat.

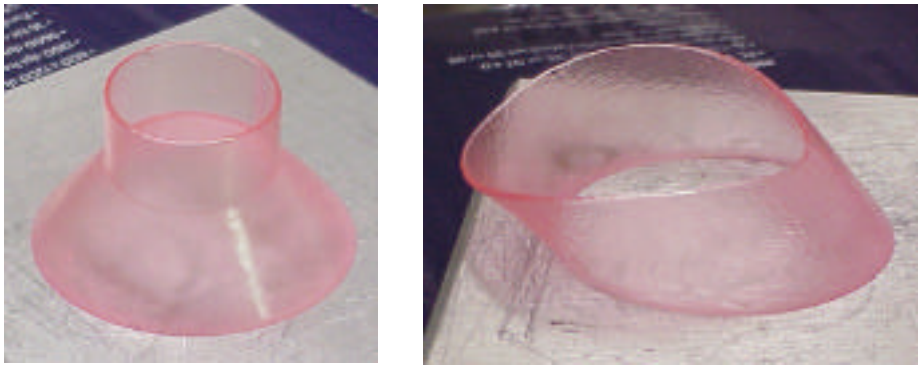

(a) (b)

Figure 9 Ice parts built by RFP process

Again, we assume that the cross-sectional profile of water deposit is circular, so the simplified model applies to the change of layer thickness of a slant wall. Figure 10 illustrates a slant wall, where Δx is the layer offset distance, $\Delta z'$ is the layer thickness of the slant wall and Δz is the layer thickness if it is built vertically. The layer thickness of a slant wall can be expressed by

$$\Delta z' = \sqrt{\Delta z^2 - \Delta x^2} = \sqrt{\frac{f \sin(\alpha/2)}{v} - \Delta x^2} \qquad (12)$$

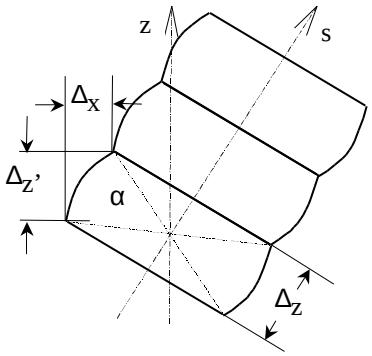

Figure 10 Slant wall

Figure 11 compares experimental data with predictions by equation (12).

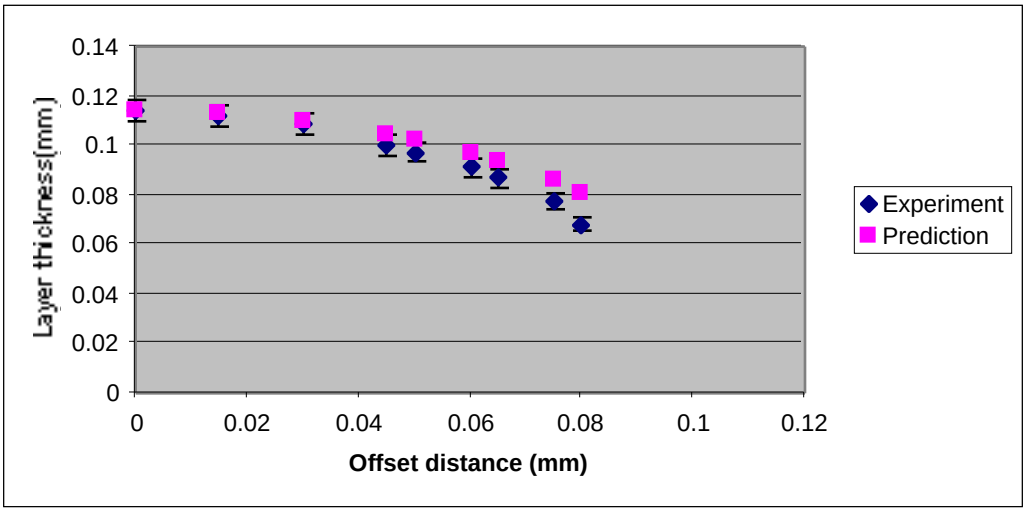

Figure 11 Layer thickness of a slant wall

During the experiment, f/v is kept constant at 0.08mm^2. Apparently, the predicted values are larger than the experimental data in a certain pattern. In the model, a new layer of water is attached to the previous layer without any impinging action, and thus water droplet is evenly distributed on the previous layer along the *s* axis. But in reality, the water droplet impinges on the previous layer at a certain speed. Due to the inertia of the droplet, the droplet will not flow

around the *s* axis evenly. It flows downward more. So the total effect is the real layer thickness along *z* direction is smaller than what the model predicted.

6. Conclusions

The governing equations of water deposit's profile in the RFP process are derived and discussed. A simplified model based on our RFP experimental conditions is proposed. The model predicts the vertical wall's layer thickness very well. If the processing parameters are kept constant, the layer thickness of a slant wall is smaller than that of a vertical wall. The relation between the layer thickness of a slant wall and the offset distance is also discussed. In order to get uniform layer thickness, water feed rate can be adjusted according to the layer offset distance during the RFP process.

7. References

[1] Zhang, W., Leu, M. C., Ji, Z., and Yan Y., "Rapid Freezing Prototyping with Water," Journal of Materials and Design, Vol. 20, June 1999.

[2] Fukai, J., Zhao, Z., Poulikakos, D., Megaridis, C., and Miyatake, O., "Modeling of the Deformation of a Liquid Droplet Impinging Upon a Flat Surface," *Physics of Fluids A,* Vol. 5, 1993.

[3] Hatta, N., Fujimoto, H., and Takuta, H., "Deformation Process of a Water Droplet Impinging on Solid Surface," Journal of Fluids Engineering, Vol. 117, 1995

[4] Chandra, S., "On the Collision of a Droplet with a Solid Surface," Proceedings of the Royal Society, Series A, Vol. 432, 1991.

[5] http://math.gmu.edu/~dmanders/, July 2000.

[6] Leu, M. C., Zhang, W., and Sui, G., "An Experimental and Analytical Study of Ice Part Fabrication with Rapid Freeze Prototyping," Annals of the CIRP, Vol. 49, No. 1, 2000.

[7] Behroozi, F., Macomber, H., Dostal, J., Behroozi, C., and Lambert, B., "The Profile of a Dew Drop," Am. J. Phys., Vol. 64, No. 9, September 1996.

[8] Dorsey, N. E., "Properties of Ordinary Water-Substance in All Its Phases: Water-Vapor, Water, and All the Ices," 1940.

[9] Hawkins, D. T., "Physical and Chemical Properties of Water: a Bibliography, 1957-1974," 1976.

[10] Neumann, A. W., Spelt, J. K., "Applied Surface Thermodynamics," 1996.

[11] Knight, C. A., "Surface Layers on Ice," J. Geophys. Res., Vol. 101, 1996.